

European XFEL SASE4-5 Workshop, 25 - 27 March 2019

Scientific Opportunities with an XFEL

Ralf Röhlsberger

Deutsches Elektronen-Synchrotron DESY, Hamburg



XFEL Parameters

XFEL @ SASE 4/5 (as given):

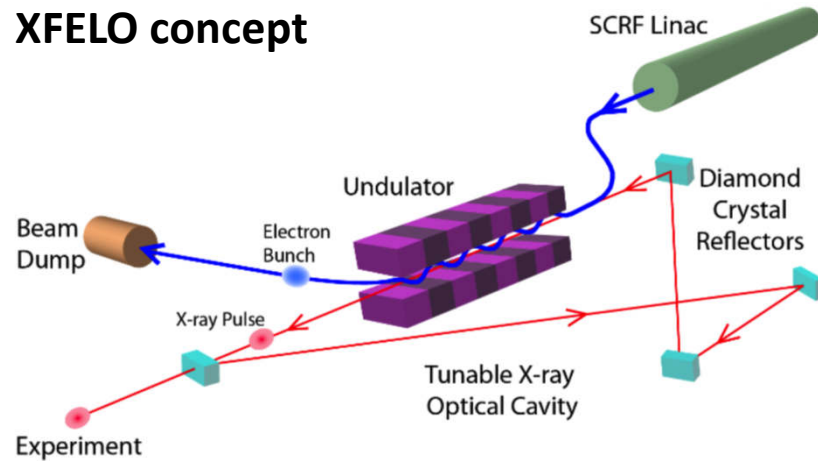
30 m undulator length

XFEL pulse energy 2.2 mJ @ 12.4 keV $\rightarrow \sim 10^{10}$ ph/meV/pulse

Bandwidth: 28 meV, Pulse length 320 fs (12 meV),

Tunability: 10^{-2} (depending on crystal arrangement)

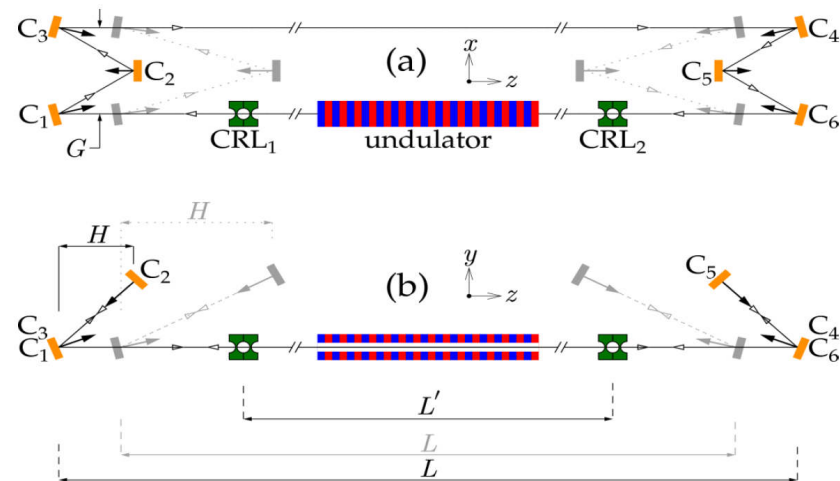
XFEL concept



Kim, Shvyd'ko, Reiche, PRL 100, 244802 (2008)

Kim, Shvyd'ko, PR-STAB 12, 030703 (2009)

Compact, non-coplanar design



Yu. Shvyd'ko, ICFA Beam Dynamics Newsletter no. 60 (2013)

Longitudinal coherence and spectral bandwidth

$$\text{Longitudinal coherence length: } \xi_L = \lambda^2 / \Delta\lambda = \lambda / (\Delta E / E) \\ \sim 100 \mu\text{m for } \Delta E / E = 10^{-6} \text{ at } 12.4 \text{ keV}$$

Small Bandwidth

→ Inelastic X-ray Scattering, Nuclear resonant scattering

Longitudinal coherence length

→ Scattering with long path-length differences, coherence at high momentum transfer

High degeneracy (all photons in the same mode)

→ multiphoton excitations, nonlinear spectroscopy, (nuclear) quantum optics

Photon degeneracy δ is the number of photons in a coherence volume, given by the transverse coherence area times the longitudinal coherence length:

$$\delta = \frac{\lambda^3}{4c} B$$

$\sim 10^9 - 10^{10}$ ph/pulse at 12.4 keV

Techniques that benefit from an XFEL source (a selection)

Inelastic nuclear resonant scattering

meV - resolved pump-probe nonequilibrium dynamics

μeV - resolved inelastic x-ray scattering: Dynamics on the mesoscale

Elastic nuclear resonant scattering

Nuclear Bragg diffraction from correlated materials

[Nuclear quantum optics](#) → [Talk by Jörg Evers](#)

High-purity X-ray polarimetry (non-nuclear)

Towards ultimate polarization purities at XFELs

Near-edge high-purity polarimetry: dichroism and birefringence

Spinwave spectroscopy

High-energy nuclear transitions (SASE-XFEL)

Probing magnetic and electronic order via ^{193}Ir → 73 keV

A source for Mössbauer spectroscopy with ^{40}K → 29.8 keV

Extreme metrology

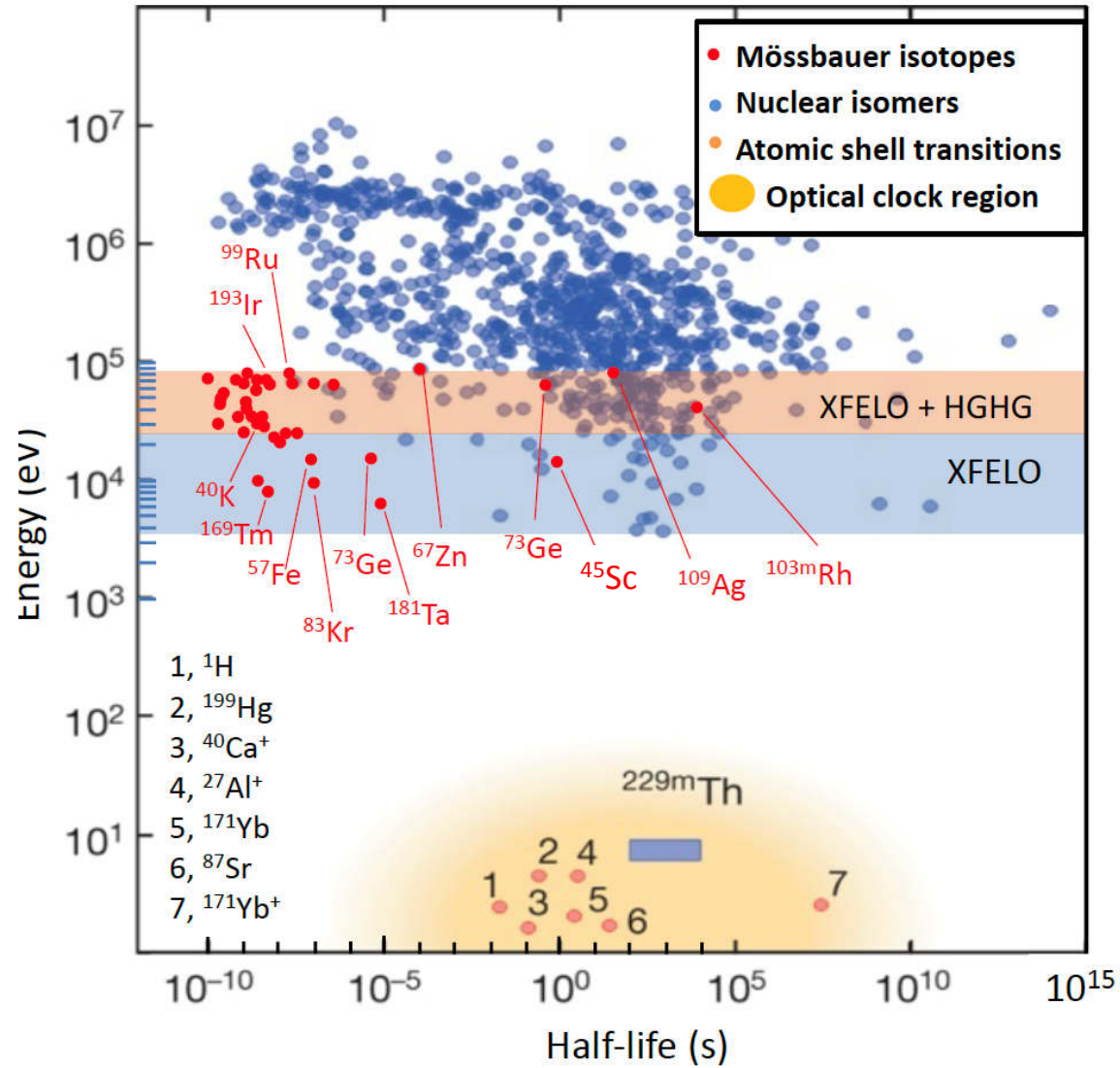
Extreme metrology with ^{229}Th → 29.2 keV

Extreme metrology with ^{45}Sc → 12.4 keV

Extreme metrology with highly charged ions (non-nuclear)

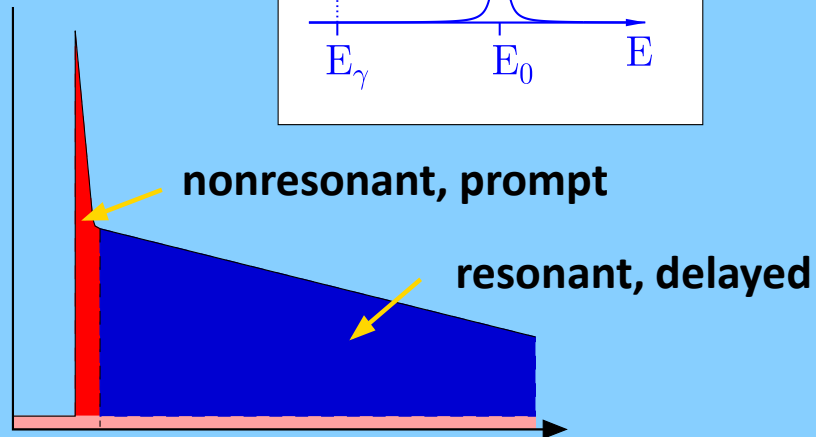
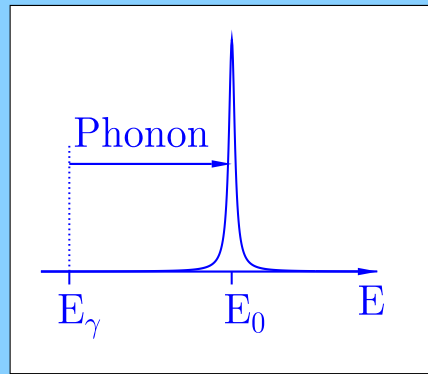
High-resolution inelastic x-ray scattering, X-ray photon correlation spectroscopy

Mössbauer Isotopes

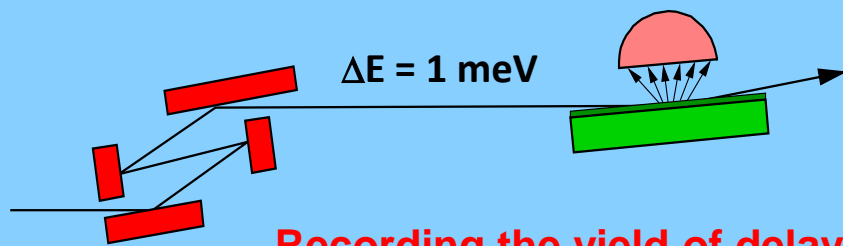


Nuclear isomer data from: von der Wense et al., Nature 533, 47 (2016)

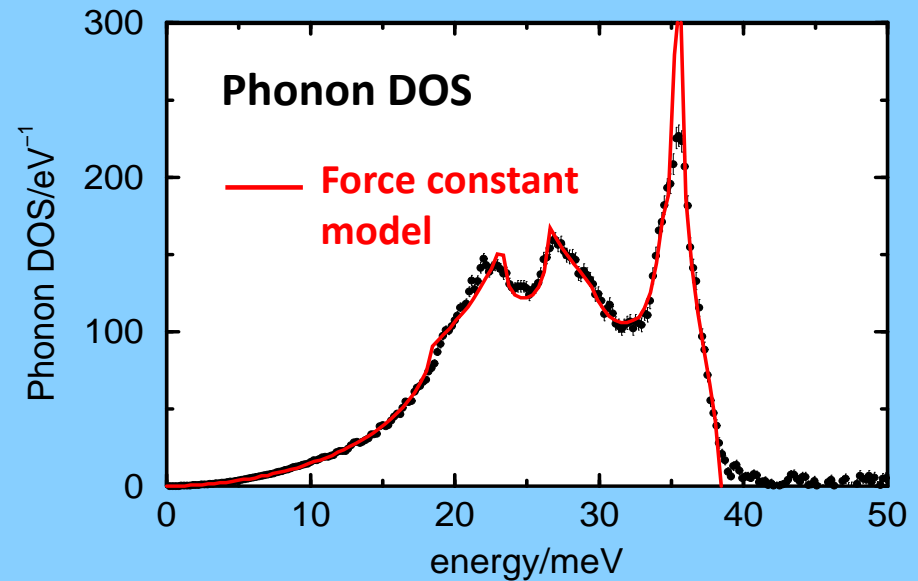
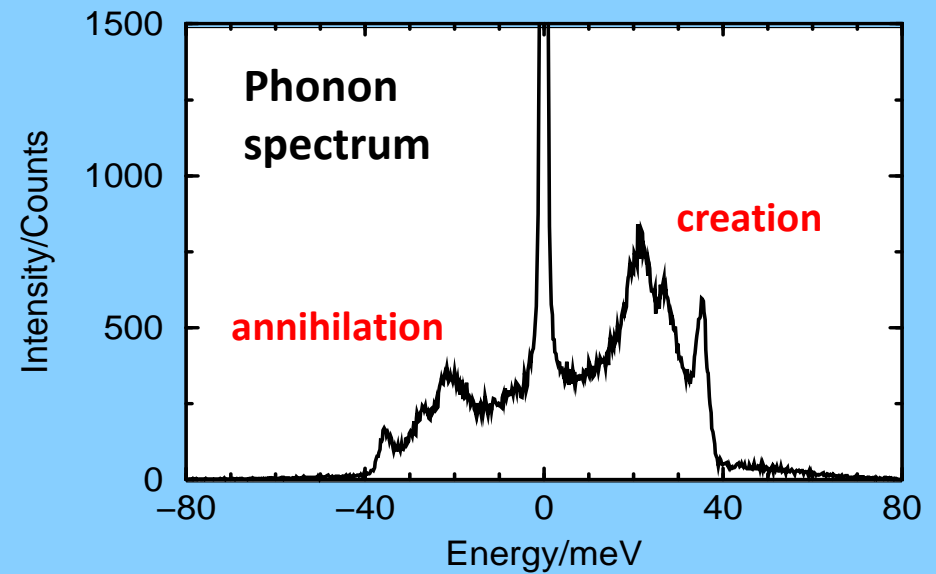
Inelastic Nuclear Resonant Scattering: The meV scale



High-resolution
monochromatization



Recording the yield of delayed
photons as function of energy

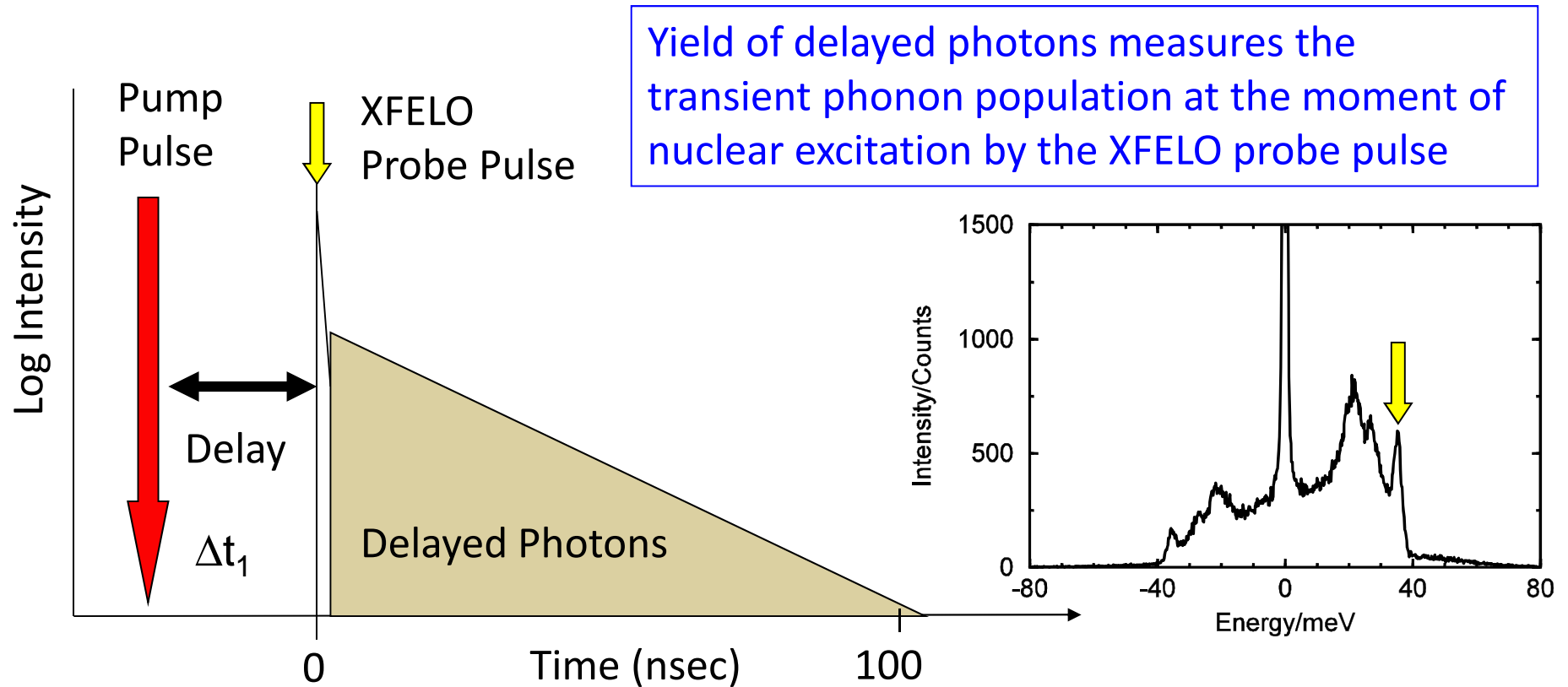


M. Seto et al. PRL 74, 3828 (1995)

W. Sturhahn et al. PRL 74, 3832 (1995)

Probing nonequilibrium phonons via nuclear excitation

meV – resolved dynamics of non-equilibrium states in condensed matter



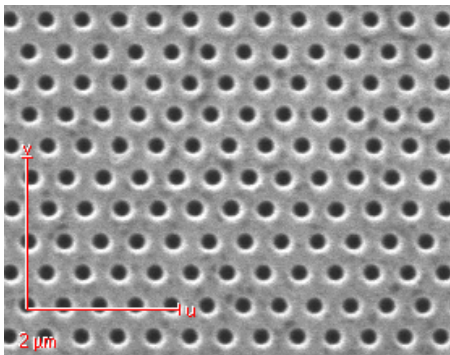
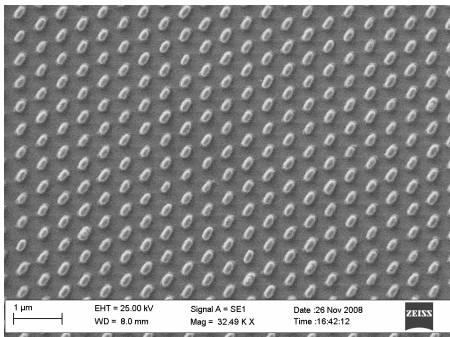
→ Probing the transient population of non-equilibrium vibrational states

G. K. Shenoy and RR,
Hyperfine Interact. 182, 157 (2008)

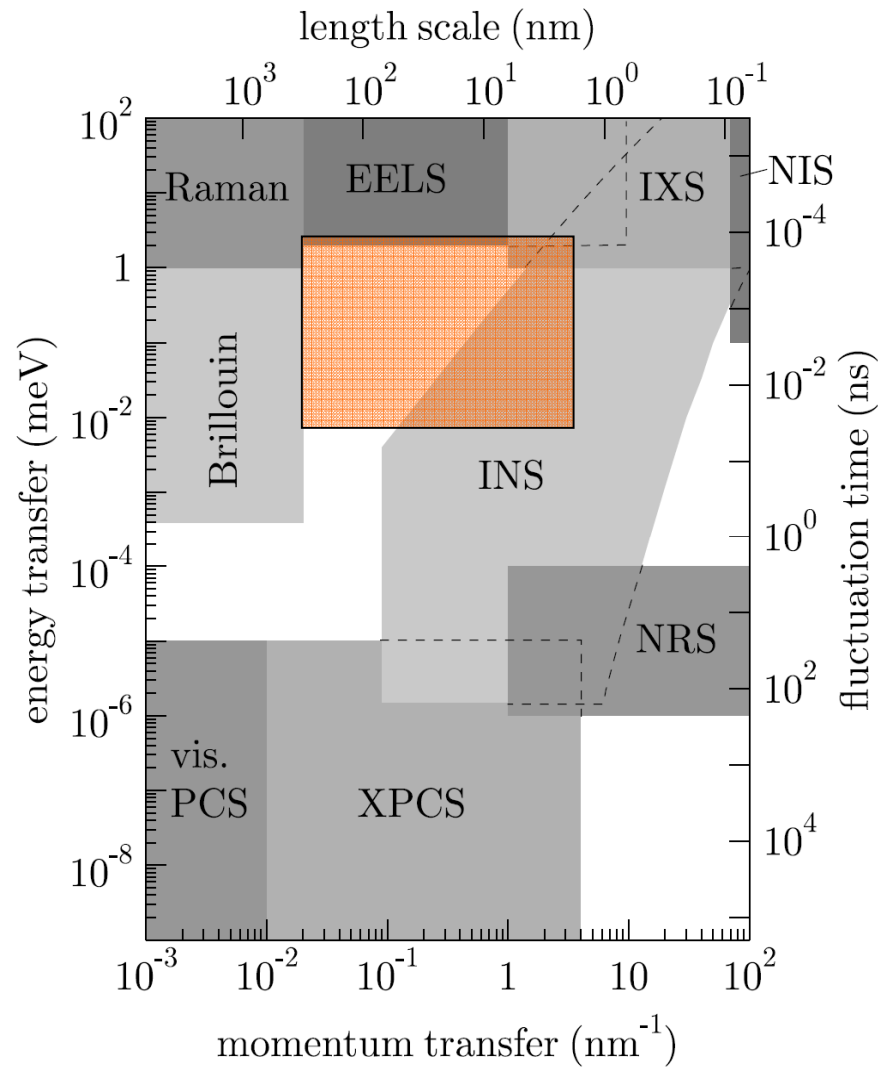
The μeV scale

Vibrational dynamics on mesoscopic length scales (1 nm – 100 nm)

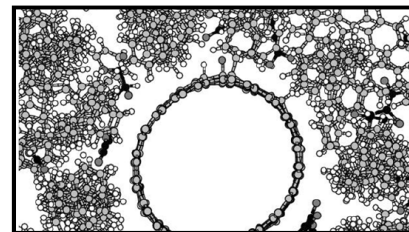
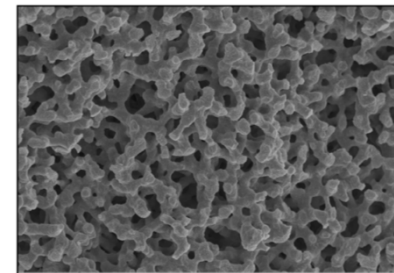
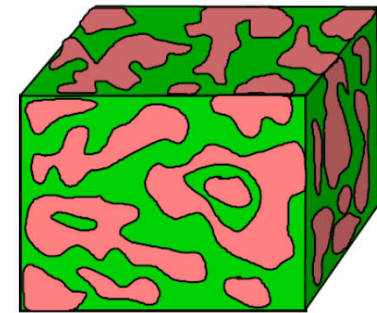
Artificially structured materials



Photonic and phononic crystals

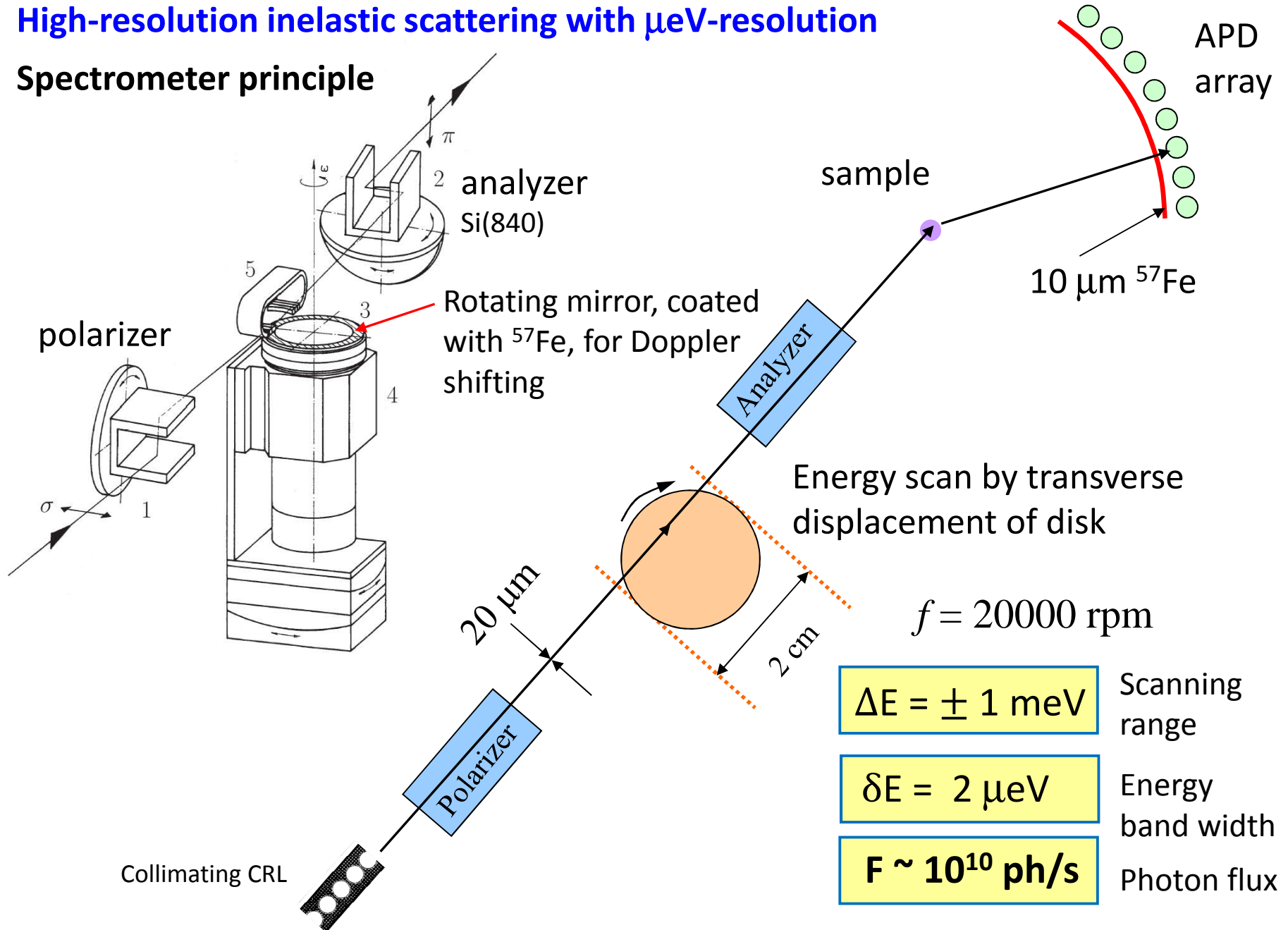


Nanocomposites

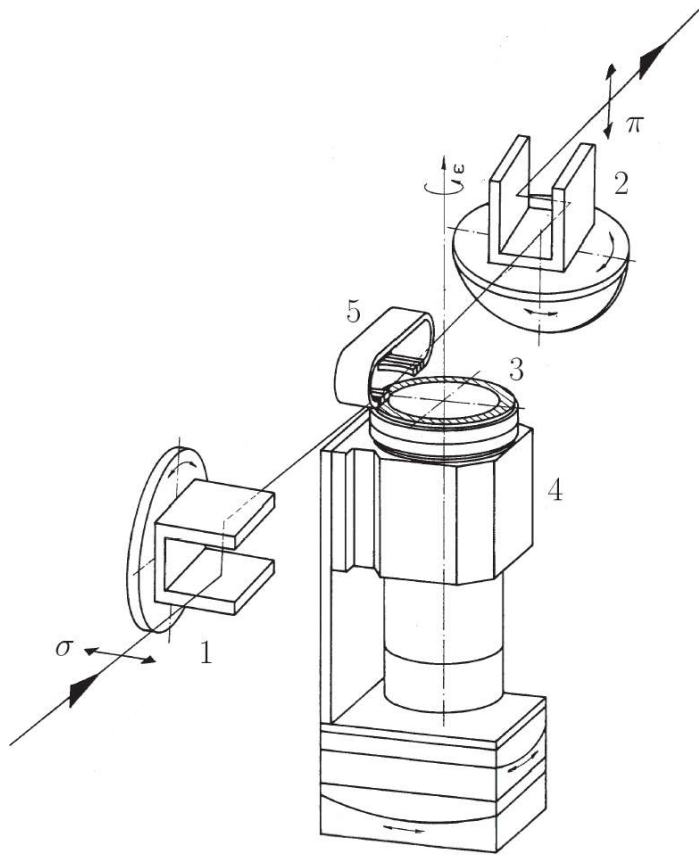


High-resolution inelastic scattering with μeV -resolution

Spectrometer principle



A MHz - XFEL would be the ideal source for this type of spectroscopy

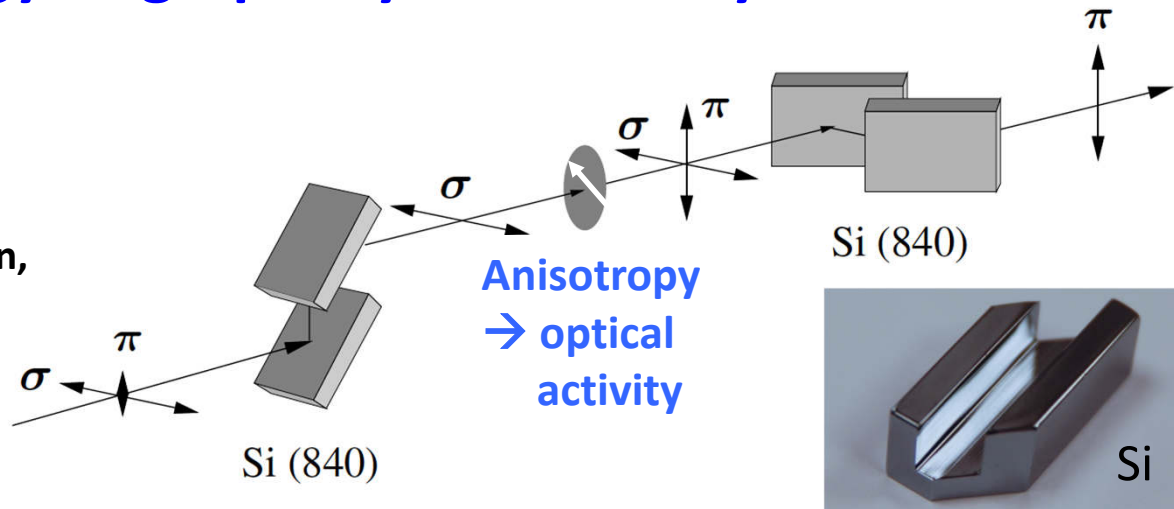


- Bandwidth of a few 10 meV matches Darwin width of reflections
- Small horizontal source size ensures high energy resolution
- Small divergence ensures high polarization purity

Enabling Technology: High-purity Polarimetry

Crossed polarizers for hard X-rays

Collaboration with I. Uschmann,
G. Paulus et al., FSU + HI Jena



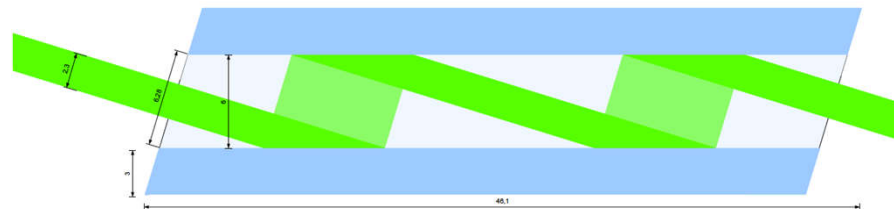
Polarization Purity

$$\delta = I_{\pi}/I_{\sigma} = 10^{-10} \dots 10^{-9}$$

- Efficient selection of $\sigma \rightarrow \pi$ scattering
- Detection of very weak anisotropies (linear, circular)

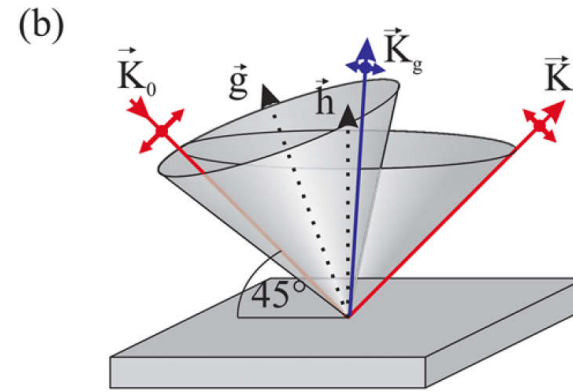
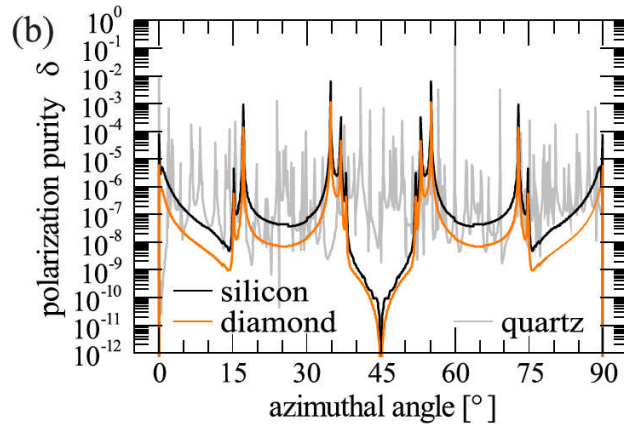
B. Marx et al.,
Opt. Commun. (2011)
Phys. Rev. Lett. (2013)
H. Bernhardt et al.,
Appl. Phys. Lett (2016)

4-bounce polarizer for 14.4 keV (B. Marx et al.)



Fundamental limitations of the polarization purity

(a) Multiple wave diffraction



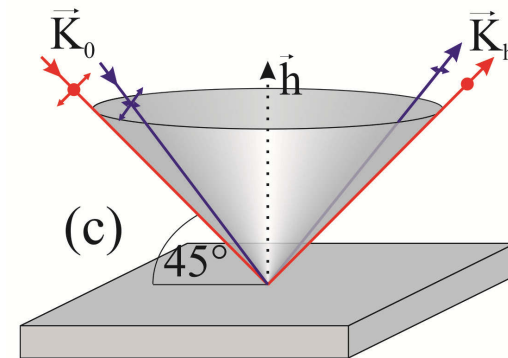
$\sigma \rightarrow \pi$ polarization transfer limits the purity for multiple reflections

(b) Beam divergence

For a Gaussian beam with H/V divergencies σ_H and σ_V :

$$\delta \approx \sigma_H^2 + \sigma_V^2 \quad \text{Polarization purity}$$

$$\delta \sim 10^{-12} \text{ for } \sigma_V, \sigma_H \sim 1 \mu\text{rad}$$



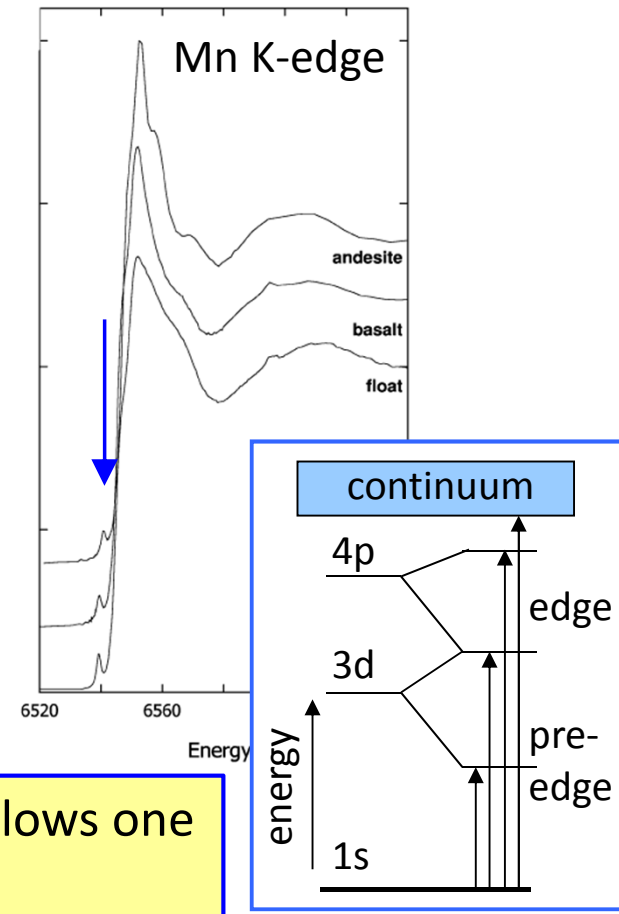
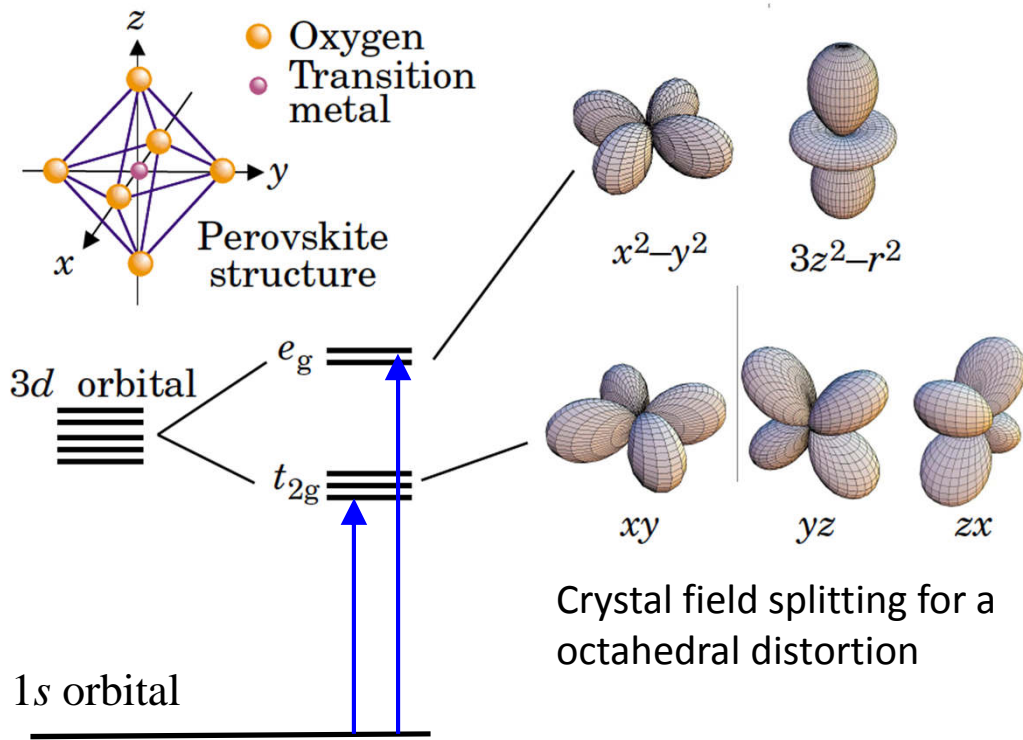
K. S. Schulze, APL Photonics 3, 126106 (2018)

Proposed detection of vacuum birefringence: T. Heinzl, R. Sauerbrey et al., Opt. Commun. 267, 318 (2006)

High-purity polarimetry: Orbital Sensitivity

Level splitting of electronic orbitals in the crystal field ...

... leads to distinct pre-edge features in the x-ray absorption spectrum
 → Strong x-ray optical anisotropy



→ Tuning the x-ray energy to pre-edge peaks allows one to probe **selected atomic orbitals**

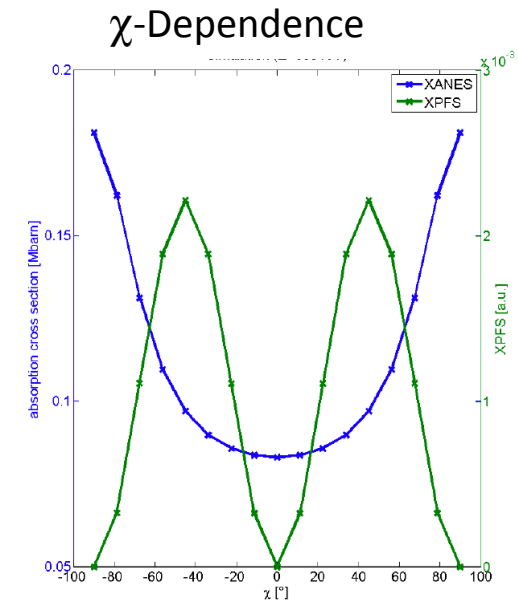
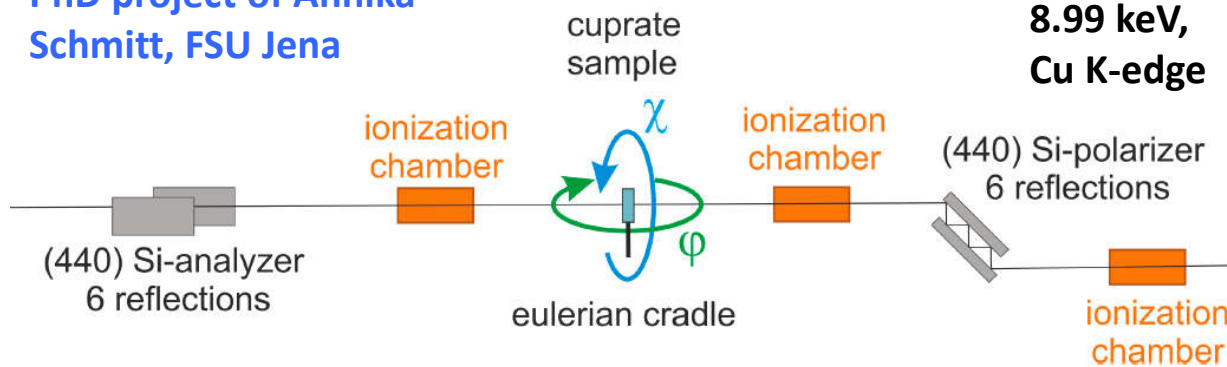
Polarizing reflections at absorption edges of transition metals (a selection)

Element	E (keV)	Crystal(hkl)	θ_B (deg)	$\Delta\theta$ (μ rad)	ΔE (meV)	$ R ^2$	Energy range (eV)
K-edges of 3d-elements							
Cu	8.979	SiO ₂ (320)	45.01	3.3	30	0.83	[-30, +32]
Fe	7.112	SiO ₂ (220)	45.19	9.2	65	0.90	[-0, +49]
		Al ₂ O ₃ (119)	44.95	3.2	23	0.81	[-30, +18]
Ni	8.347	SiO ₂ (015)	45.14	6.5	54	0.89	[-8, +50]
V	5.465	Al ₂ O ₃ (116)	45.12	13.0	70	0.90	[-7, +30]
Cr	5.989	Al ₂ O ₃ (117)	45.03	5.6	33	0.79	[-16, +24]
Mn	6.541	Al ₂ O ₃ (302)	44.89	6.7	44	0.87	[-38, +7]
L-edges of 4f-elements							
Ce L ₂	6.164	SiO ₂ (300)	45.15	5.9	36	0.63	[-5, +37]
Pr L ₂	6.440	Si(400)	45.15	24.7	160	0.95	[-5, +39]
Eu L ₂	7.617	SiO ₂ (131)	44.89	5.9	45	0.85	[-40, +12]
	L ₃	6.977	SiO ₂ (302)	45.02	10.6	74	0.89
Gd L ₂	7.930	Si(422)	44.84	14.4	115	0.96	[-49, +5]
L-edges of 5d-elements							
Ir L ₃	11.215	Si(444)	44.84	5.0	57	0.96	[-70, +7]
W L ₃	10.207	Si(620)	45.01	6.8	70	0.96	[-33, +37]
	L ₂	11.544	Si(711)	44.92	3.2	38	0.91

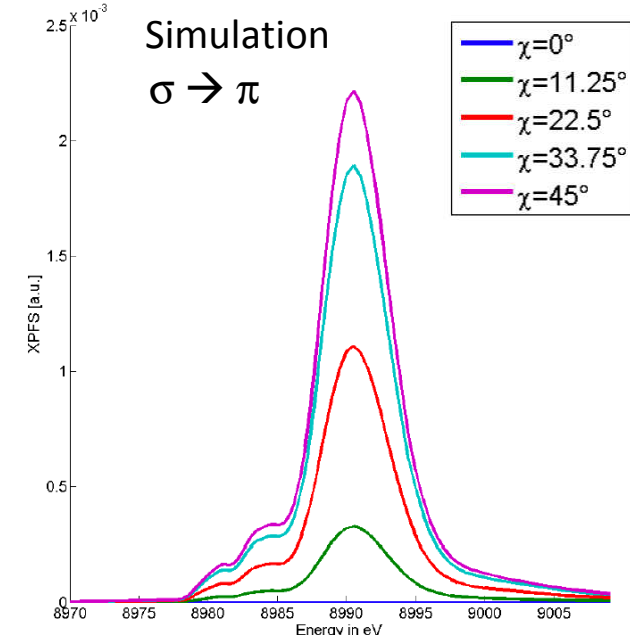
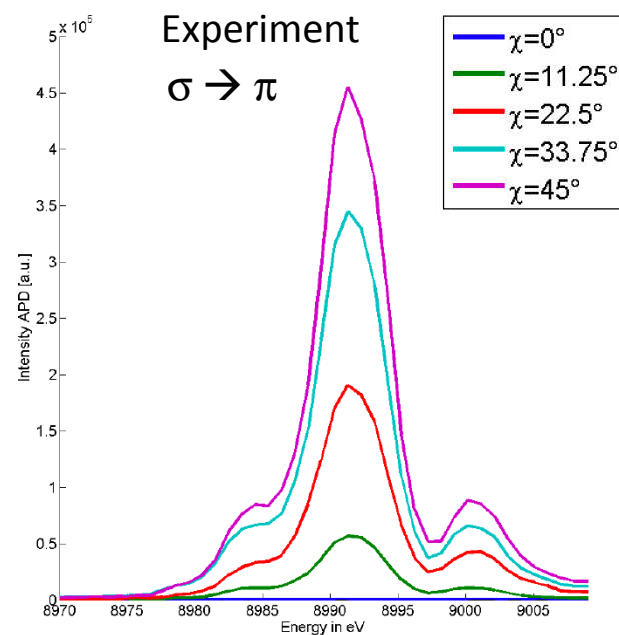
X-ray Spectro-Polarimetry on La_2CuO_4 (LCO)

LCO: mother-compound of high- T_c superconductors,
e.g., $\text{La}_{2-x}\text{Sr}_x\text{CuO}_4$

PhD project of Annika
Schmitt, FSU Jena



Sample preparation:
Jerome Debray,
CNRS Grenoble
DFT Simulations:
Yves Joly,
Institut Neel, Grenoble

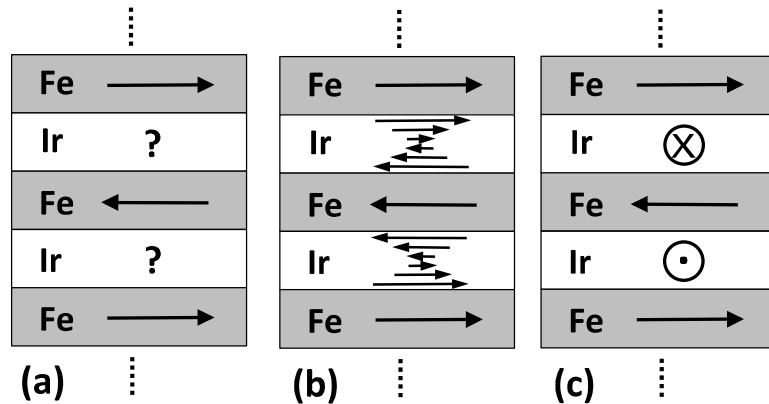


Induced 5d Magnetic Superstructures in Fe/Ir Multilayers

PhD project of Benjamin Grabiger, FSU Jena

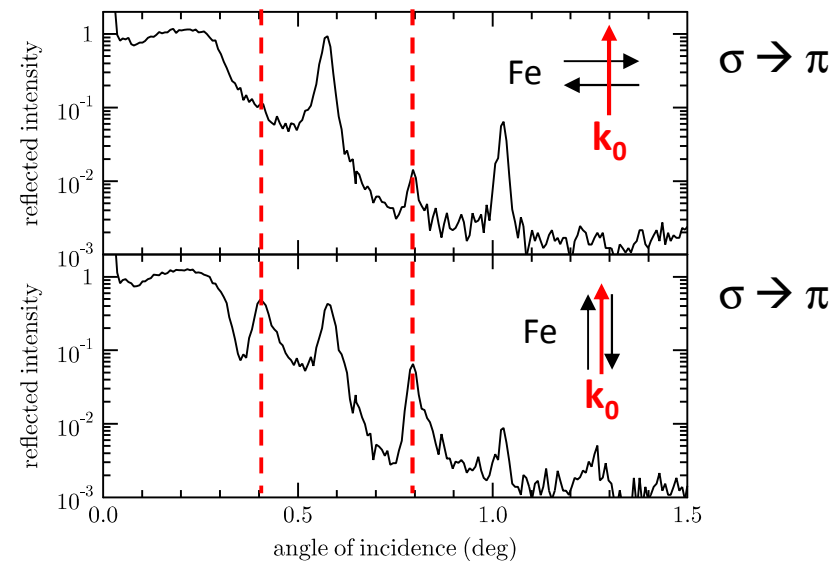
Multilayers of ferromagnetic 3d metals and non-magnetic 5d elements
 → promising candidates for the next generation of magneto-optic recording media.

How do ferromagnetically ordered Fe layers influence adjacent Ir layers?



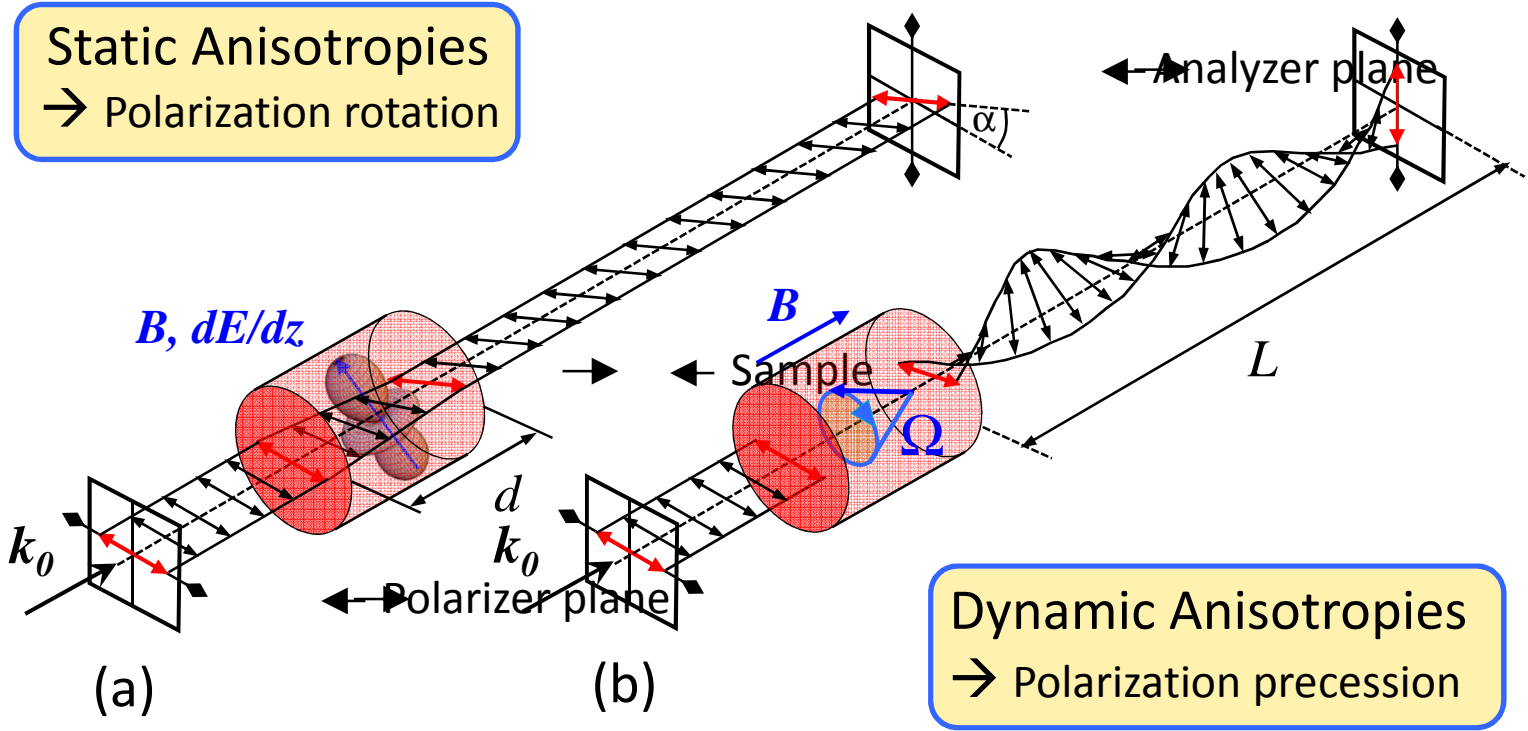
Multilayer with antiferromagnetic alignment of Fe layers, produced at DESY via **oblique incidence deposition (OID)**.

Magnetic superstructure of Fe is imprinted into the Ir !



Experiment performed via high-purity polarimetry at the **L₃ edge of Ir at 11.2 keV**

Probing Tiny Anisotropies in Condensed Matter via High-Purity Polarimetry



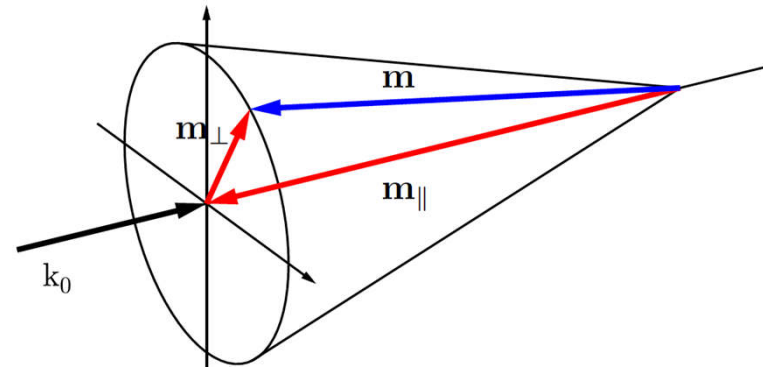
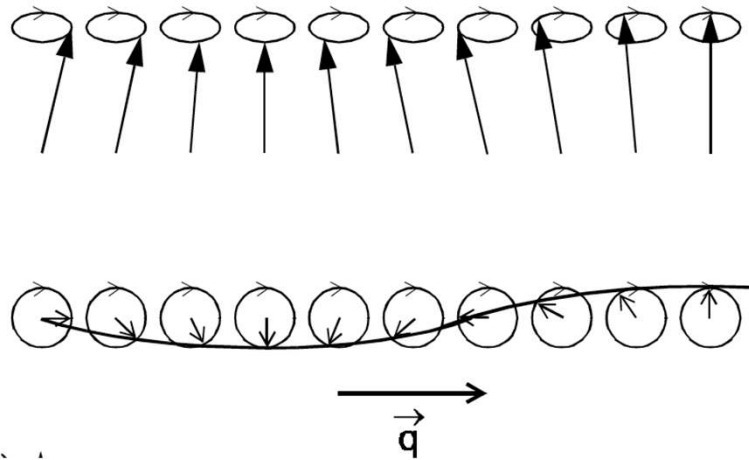
Probing charge anisotropies in correlated materials
 → Addressing selected orbitals via resonant x-rays

Probing spin excitations in magnetic materials
 → PRL 112, 117205 (2014)

Magnons (Spinwaves)

Magnetization causes rotational anisotropy in solids

Dynamic anisotropy in spin waves:



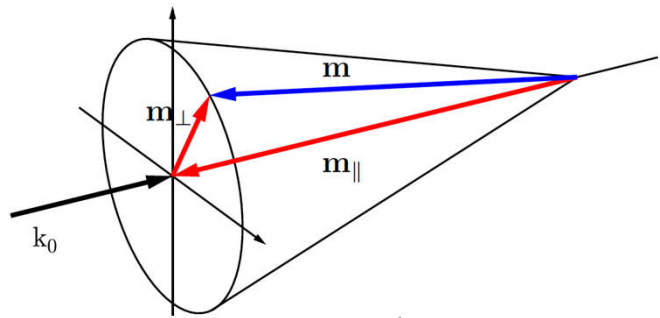
Resonant Scattering from Magnons: Twisted Polarization

$$\begin{bmatrix} \square \\ \square \end{bmatrix} A_{S_{circ}} \begin{bmatrix} \square \\ \square \end{bmatrix} = i e^{j 2\Omega t} A_{-} + e^{-j 2\Omega t} A_{+}$$

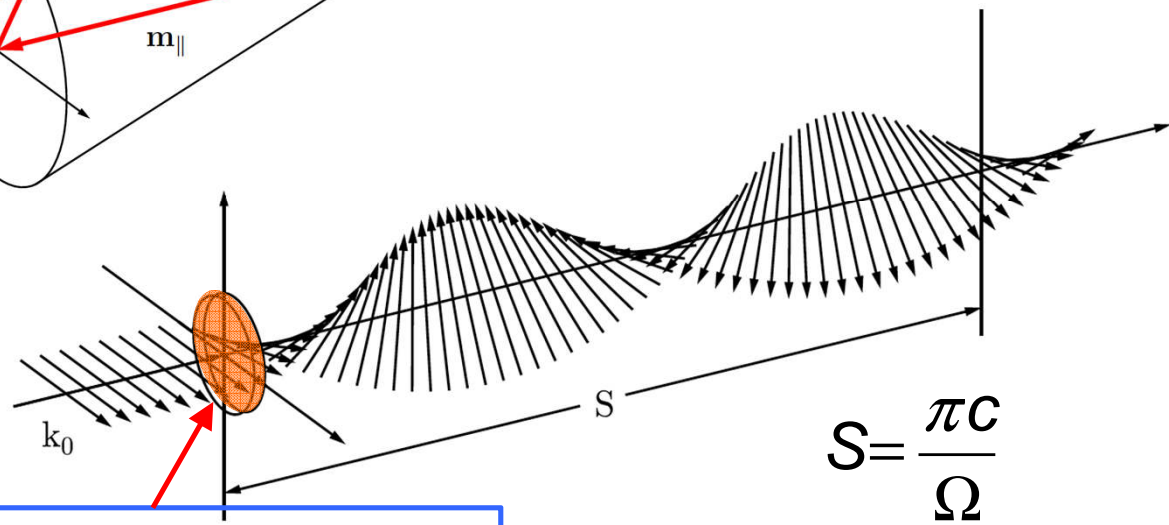
Transmission through a rotating half-wave plate / Light scattering from a magnon

Transformation into linear basis:

$$\begin{bmatrix} \square \\ \square \end{bmatrix} A_{S_{lin}} \begin{bmatrix} \square \\ \square \end{bmatrix} = \cos 2\Omega t A_{H} - \sin 2\Omega t A_{V}$$



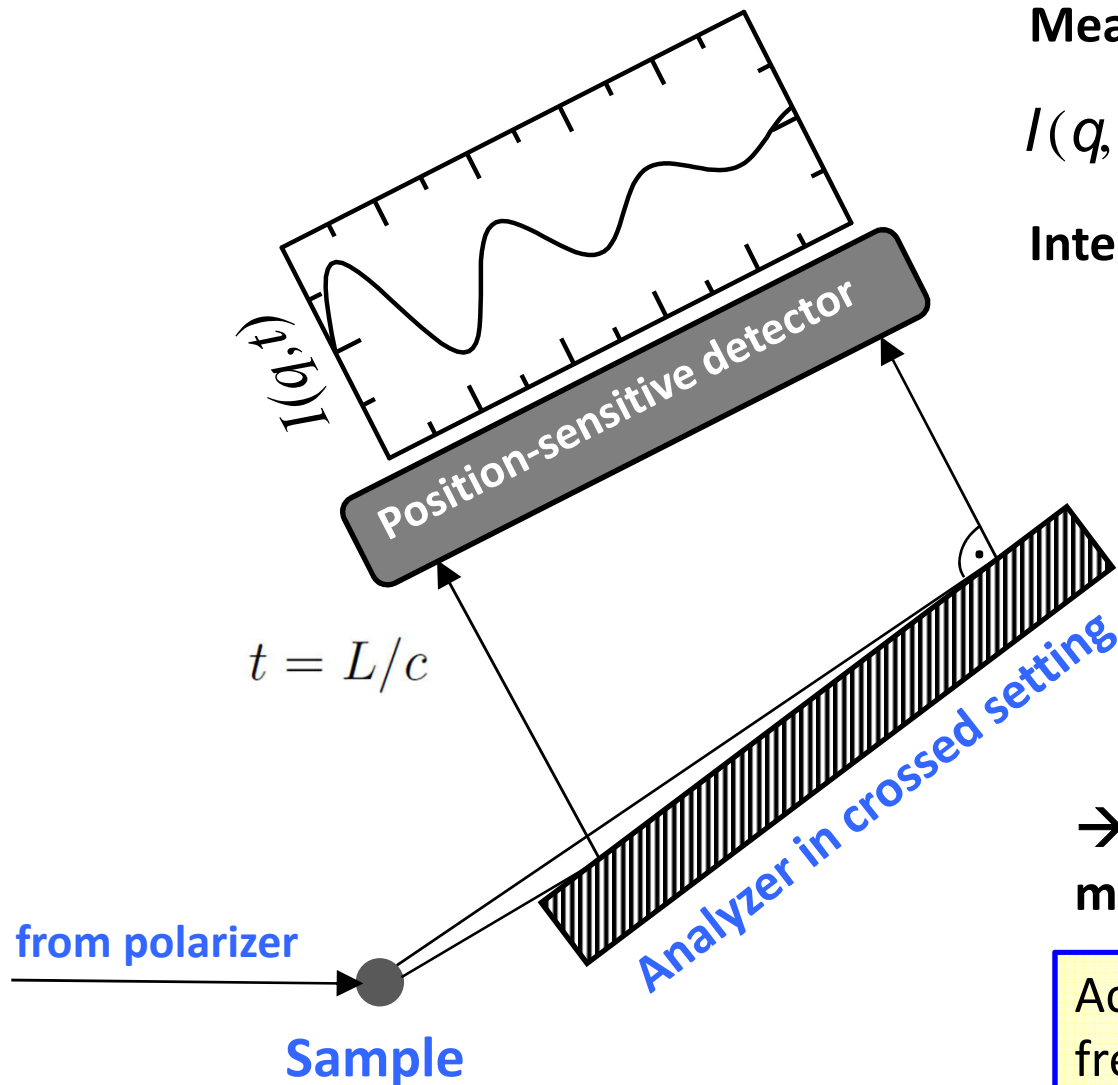
Polarization precession in space



$$S = \frac{\pi C}{\Omega}$$

Sample with magnon excitation

Resonant Scattering from Magnons: Polarization Analysis



Measured signal:

$$I(q,t) = I_B + I_0 \int S(q,\Omega) \cos 2\Omega t d\Omega$$

Intermediate scattering function

- Compare with Neutron Spin Echo
- Energy transfer encoded in polarization
- **Independent of energy bandwidth !**

→ Probing low-energy magnetic excitations

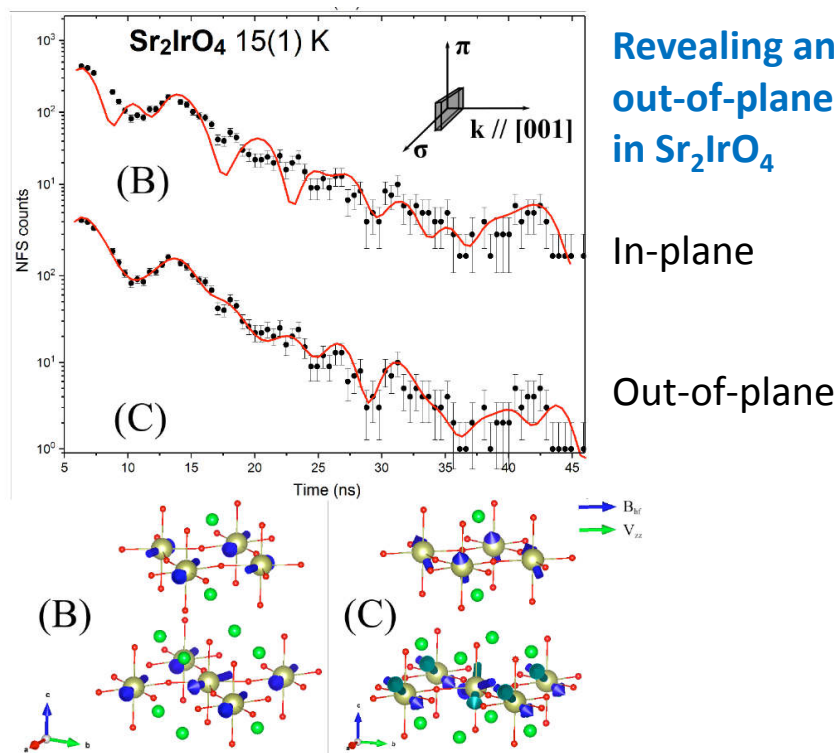
Accessible range of spinwave frequencies: 1 – 500 GHz

Probing magnetic and electronic order at 73 keV via ^{193}Ir

SCIENTIFIC REPORTS 9, 5097 (2019)

Nuclear resonant scattering from ^{193}Ir as a probe of the electronic and magnetic properties of iridates

Pavel Alexeev^{1,2}, Olaf Leupold¹, Ilya Sergueev¹, Marcus Herlitschke¹, Desmond F. McMorro³, Robin S. Perry³, Emily C. Hunter³, Ralf Röhlsberger¹, and Hans-Christian Wille^{1*}



Revealing an anomalous out-of-plane spin structure in Sr_2IrO_4

In-plane

Out-of-plane

High-energy XFEL-SASE

- Access to absorbing sample environments
- Study magnetic and electronic phase transitions in correlated materials under extreme conditions

A source for Mössbauer spectroscopy with ^{40}K

Transition energy: 29.8 keV
 Lifetime: 8 ns
 Natural abundance: 0.01 %

Relevant for:

- biological functions
- unconventional superconductors

Requires extension of polarimetry to high energies !

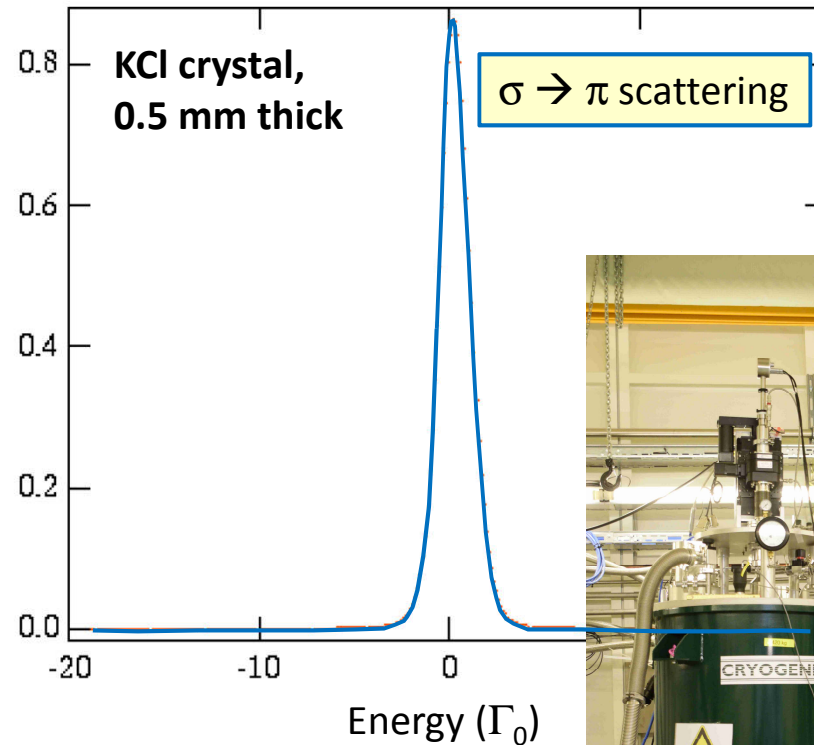
Potential reflections:

^{40}K , $E = 29.834$ keV, $\tau = 5.96$ ns

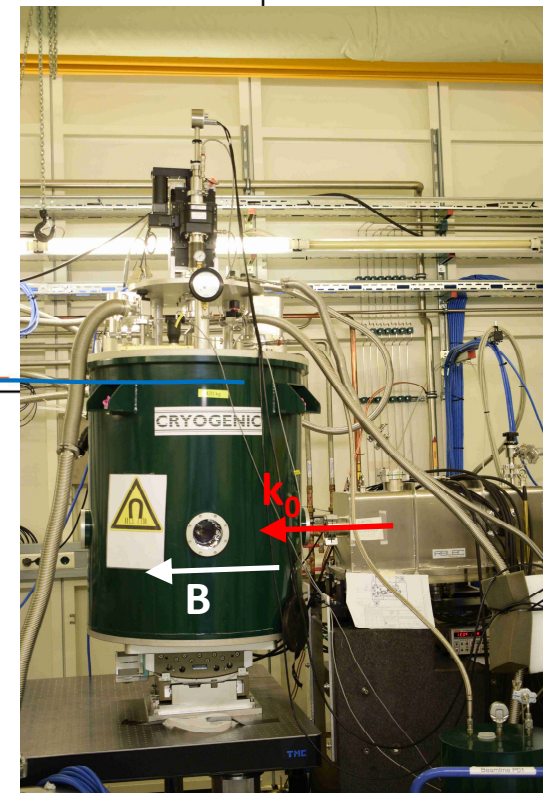
Diamond

0	0	12	44.35285	93.54033	0.03479	0.00106	0.943
11	5	1	44.93625	90.37952	0.02309	0.00069	0.932

6 T magnetic field in Faraday geometry

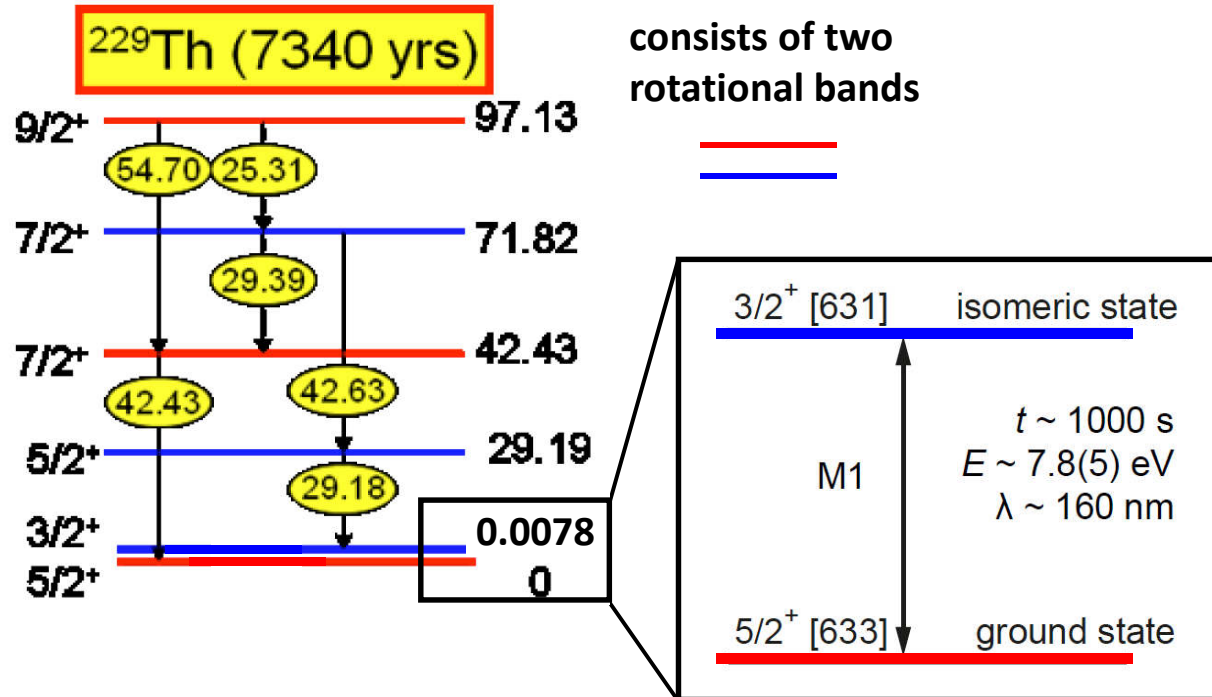


BMBF
 Verbund
 projekt
 FSU Jena



The quest for the ultimate (nuclear) frequency standard

The case of ^{229m}Th



Nuclide	^{229}Th
Abundance, (%)	7340 yrs (100%)
Resonance, E_0	7.6 eV
Transition ($I_g - I_e$)	$5/2^+ - 3/2^+$
Multipolarity	M1
$T_{1/2}$	26,000 s
Bandwidth, Γ	17.5 zeV

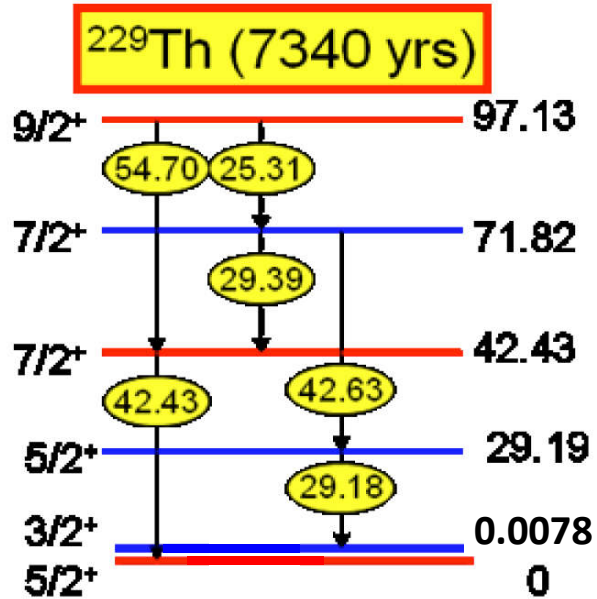
$$Q = \Gamma/E_0 = 2.3 \times 10^{-21}$$

- B. R. Beck et al., PRL 98, 142501 (2007)
 S. Stellmer et al. J. Phys. Conf. Ser. 723, 012059 (2016)
 L. von der Wense et al., Nature 533, 47 (2016)

The quest for the ultimate (nuclear) frequency standard

The 7.8(5) eV transition in ^{229m}Th

$$Q = \Gamma/E_0 = 2.3 \times 10^{-21}$$



Applications

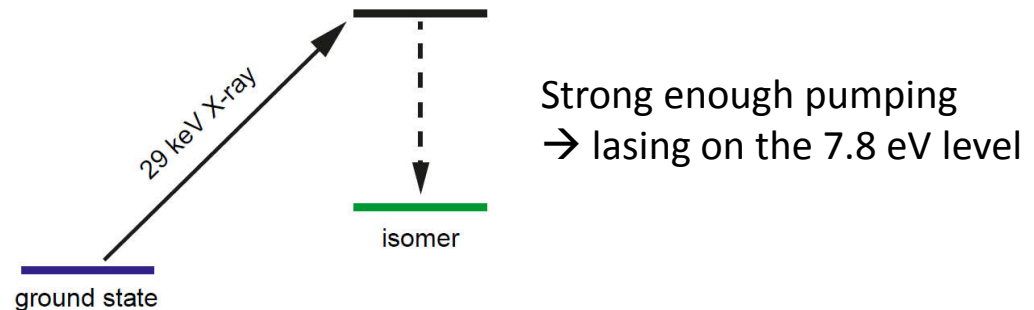
- Extreme-precision tests of relativity
- Variation of fundamental constants
- Qubits for quantum computing

XFEL contribution:

- Exact determination of transition energy E_0 with meV accuracy: $E_0 = (29.39 + 42.43 - 42.63 - 29.18)$ keV
- Population of the 7.8 eV level via excitation of the 29.19 keV level (200 ps lifetime)

Platforms:

- Trapped ions
- doped CaF_2 crystals



Towards x-ray frequency combs

Distinguishing feature of the XFEL: Pulses are recirculating

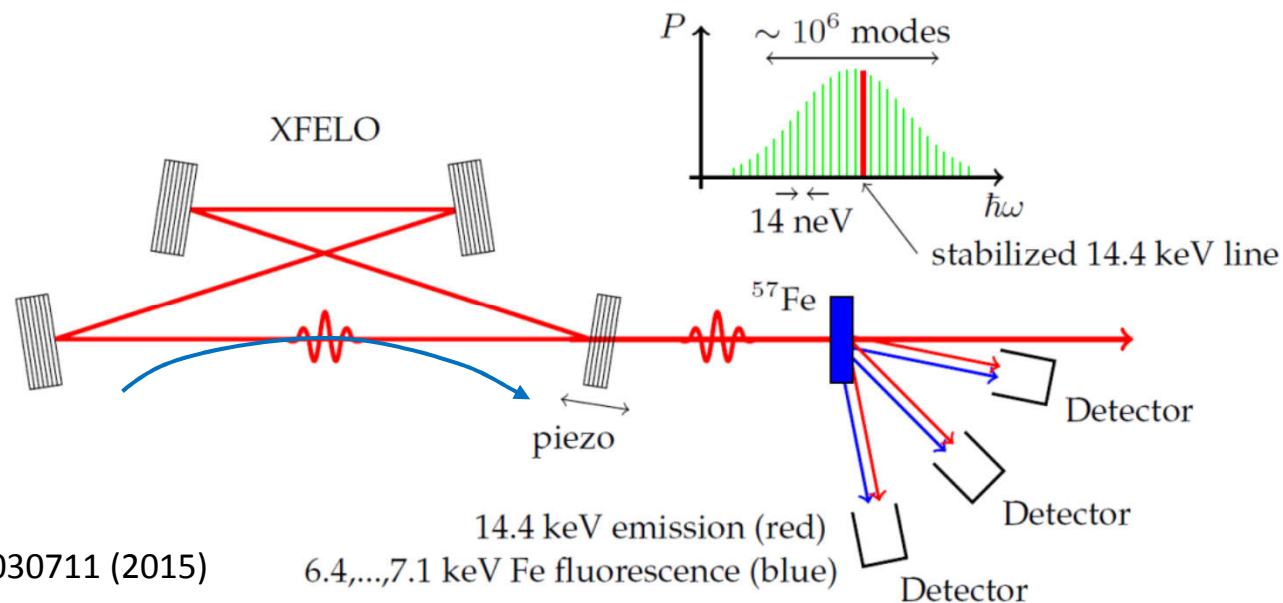
→ Output pulses are coherent if the cavity length is kept stable

→ Output spectrum consists of sharp lines spaced by $h/T_e \sim 10 - 20$ neV

Fluctuating cavity length, spont. emission noise and phase errors accumulate

→ Comb lines broaden, interpulse coherence is lost

→ **Locking cavity length to an external reference, e.g., nuclear resonance**



The 12.4 keV resonance of ^{45}Sc

Linewidth: $\Gamma_0 = 10^{-15}$ eV (1 feV)
 Half-life: $\tau_0 = 300$ ms
 Natural abundance: 100 %

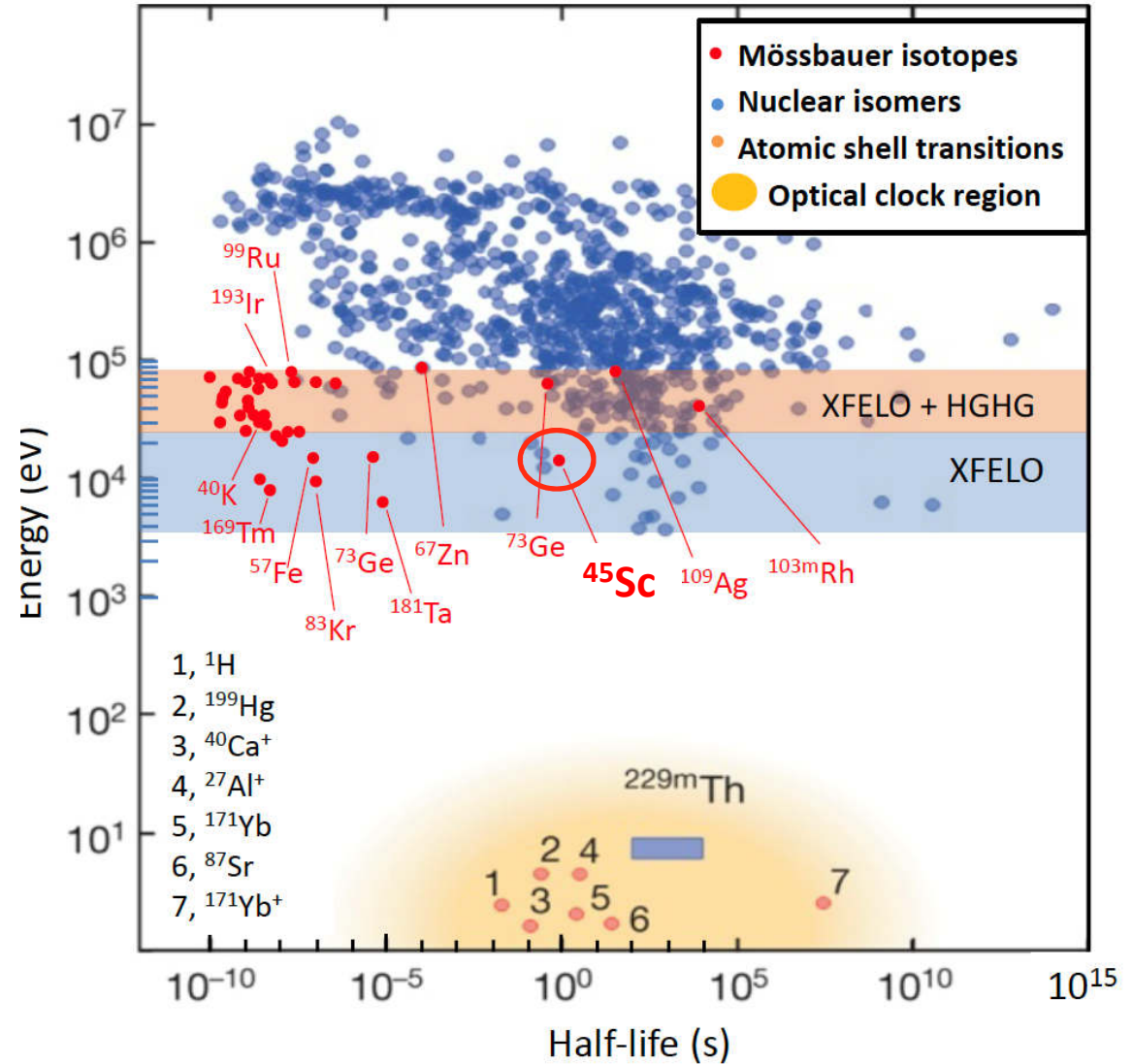
Spectral flux of SASE-XFEL

$$3 \times 10^3 \text{ ph/s/feV}$$

Spectral flux of XFELO

$$3 \times 10^5 \text{ ph/s/feV}$$

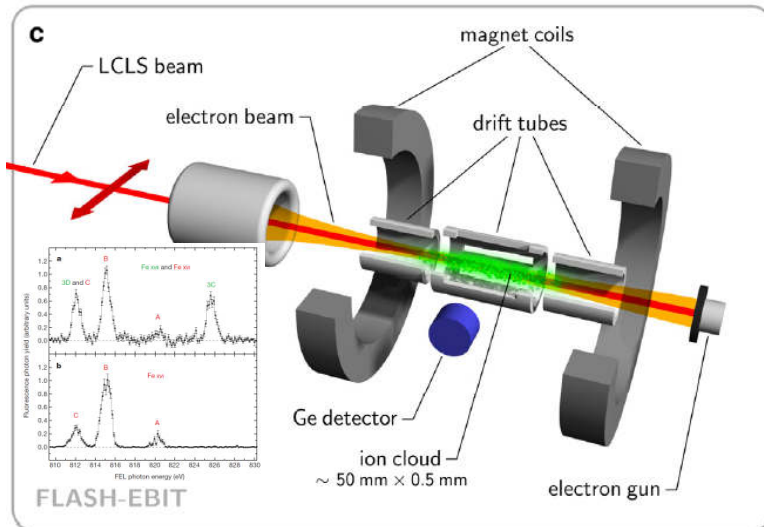
$$\Gamma_0/E_0 = 10^{-19}$$



Nuclear isomer data from: von der Wense et al., Nature 533, 47 (2016)

Towards x-ray precision metrology of highly-charged ions

image (modified) from:
Bernitt *et al.* Nature (2012) , **Crespo group at MPIK, Heidelberg**



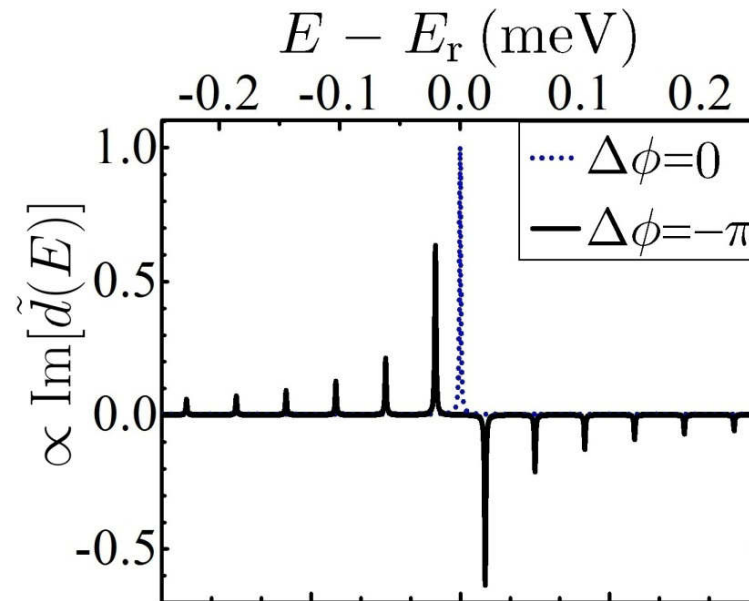
High-resolution spectroscopy of long-lived transitions in highly-charged ions:

- Precision tests of theory in heavy ions (QED, nuclear, relativistic-electronic structure)
- linking nuclear/electronic x-ray transitions: variation of fundamental "constants" ?

Coulomb crystallization of highly charged ions Science 347, 1233 (2015)

L. Schmöger,^{1,2} O. O. Versolato,^{1,2*} M. Schwarz,^{1,2} M. Kohnen,² A. Windberger,¹
B. Piest,¹ S. Feuchtenbeiner,¹ J. Pedregosa-Gutierrez,³ T. Leopold,²
P. Mücke,^{1,2} A. K. Hansen,^{4,†} T. M. Baumann,⁵ M. Drewsen,⁴ J. Ullrich,²
P. O. Schmidt,^{2,6} J. R. Crespo López-Urrutia^{1,‡}

Courtesy of Thomas Pfeifer



Summary

Develop the XFEL concept towards a meV-bandwidth x-ray source with outstanding spectral/longitudinal coherence properties

Fascinating scientific applications

- High-resolution ($\mu\text{eV} - \text{meV}$) inelastic x-ray scattering for non-equilibrium vibrational dynamics on all length scales
- Spectropolarimetry with highest purity of static and dynamic anisotropies in correlated materials with orbital sensitivity
- Multiphoton- and nonlinear optics towards quantum optics and coherent control
- Extreme metrology with nuclear resonances and highly charged ions

Technical prerequisites have been provided:

- ✓ High-reflectivity diamond crystals
- ✓ Heat-load tests of diamond crystals
- ✓ Nano-radian angular stabilization of crystal arrangements

Next step(s): **Demonstration of gain** (and generate funds for it)